

Ferroelectric properties in all solution prepared $\text{Bi}_6\text{Fe}_2\text{Ti}_3\text{O}_{18}/\text{Ba}_{0.92}\text{La}_{0.08}\text{SnO}_3$ thin films

Li Zhang^{*,†}, Yibao Li^{*}, Zhen Tang^{*}, Yan Deng^{*}, Hui Yuan^{*},
Jiangying Yu^{*} and Xuebin Zhu[†]

^{*}Department of Mathematics and Physics,
Anhui Jianzhu University, Hefei 230022, China

[†]Key Laboratory of Materials Physics, Institute of Solid State Physics,
Chinese Academy of Sciences, Hefei 230031, China

[†]lizhang@ahjzu.edu.cn

Received 7 June 2016

Revised 10 September 2016

Accepted 3 October 2016

Published 7 December 2016

In this paper, all solution processing is used to prepare both the transparent conducting $\text{Ba}_{0.92}\text{La}_{0.08}\text{SnO}_3$ (BLSO) thin films as bottom electrodes and ferroelectric $\text{Bi}_6\text{Fe}_2\text{Ti}_3\text{O}_{18}$ (BFTO) thin films. The derived BFTO thin films are characterized by X-ray diffraction (XRD) and field-emission scanning electron microscopy (FE-SEM). The derived thin film is polycrystalline with dense microstructures. The remnant polarization $2P_r$ at the measurement frequency of 2 kHz can reach $\sim 16.8 \mu\text{C}/\text{cm}^2$ under the 500 kV/cm electric field and the coercive field $2E_c$ is 410 kV/cm. The results will provide a feasible route to prepare BFTO thin films on transparent conducting bottom electrodes to realize multifunctionality.

Keywords: Chemical solution deposition; film; ferroelectric.

1. Introduction

Layered Bi-containing Aurivillius phases as one important series of ferroelectric materials have been widely investigated due to the excellent properties such as large polarizations and environment-friendly (Pb-free) behaviors.^{1–3} $\text{Bi}_6\text{Fe}_2\text{Ti}_3\text{O}_{18}$ (BFTO) as a typical layered Bi-containing Aurivillius phase has been studied because of its high ferroelectric Curie temperature ($T_c \sim 1075 \text{ K}$).^{4,5} Currently, several methods have been used to fabricate BFTO thin films.^{6–10} Chemical solution deposition (CSD) as a typical route for thin films preparation has been also widely used to deposit BFTO thin films.^{6–15} Currently, the BFTO thin films are usually deposited on platinized silicon wafers. In view of applications, BFTO thin films are desirable to deposit on different substrates such as on transparent conducting oxide

(TCO) buffered wafers to realize multifunctionality.¹⁶ Till now, there has no report about BFTO thin films on transparent conducting wafers.

Considering the relatively high annealing temperature of BFTO thin films in CSD processing, the commonly used TCOs such as SrTiO₃ and ZnO cannot be used as the bottom electrodes due to the degradation at high temperatures. It is desirable to explore suitable TCOs as the bottom electrodes for BFTO thin films. Moreover, to realize the all solution route for large-area BFTO thin films, the TCO bottom electrodes should be also prepared by CSD. In the few past years, La-doped BaSnO₃ shows high electrical mobility and low electrical resistivity at room-temperature.^{17–22} Moreover, the La-doped BaSnO₃ is robust at high temperatures.¹⁷ Currently, La-doped BaSnO₃ thin films have been successfully prepared by several types of routes. Amongst, the La-doped BaSnO₃ thin films derived by CSD show relatively excellent properties, indicating the feasibility to realize all solution processing of BFTO thin films on TCO bottom electrodes.^{23,24}

In this paper, ferroelectric BFTO thin films have been deposited on transparent conducting La-doped BaSnO₃ thin films by an all solution method. The results show that the derived BFTO thin films are polycrystalline, and the ferroelectric properties are comparable with the BFTO thin films on platinized silicon wafers. The results will provide an effective route to realize the BFTO based thin films on TCO bottom electrodes by an all solution method.

2. Experimental Study

Ba_{0.92}La_{0.08}SnO₃ (BLSO) thin films were prepared by CSD method on LaAlO₃ (LAO, 001) substrates as our previous report usage of the solution concentration of 0.4 M in BLSO stoichiometry.²³ BFTO thin films were also prepared by CSD. The precursor solution was prepared using bismuth acetate, iron acetate and tetrabutyl titanate as starting materials and propionic acid as solvent. A 10%mol excess Bi acetate was used to compensate the volatilization of Bi element in processing. The used solution concentration was of 0.1 M in BFTO. The BFTO thin films were spin-coated onto the prepared BLSO/LAO substrates and baked at 350°C for 10 min in air, and the spin-coating and baking processing were repeated for several times to increase the thickness. Finally, the baked thin films were annealed at 700°C for 30 min in air by rapid thermal annealing processing.

The microstructures were analyzed by X-ray diffraction (XRD) using Cu K_α radiation and field-emission scanning electron microscopy (FE-SEM). The temperature dependence of the resistivity $\rho-T$ of the derived BLSO/LAO thin films was measured on a physical property measurement system (PPMS) using the four-probe method. The room-temperature Hall measurements of the derived BLSO/LAO thin films were also carried out on PPMS using the van der Pauw geometry. Top Au electrodes of 0.2 mm in diameter were deposited by a small ion sputtering equipment (SBC-12, KYKY, Beijing) onto the BFTO surface through a shadow mask. The ferroelectric and the leakage properties were investigated using a Sawyer-Tower

circuit attached to a computer-controlled standardized ferroelectric test system (Radiant Precision Premier II, Radiant Technologies, USA).

3. Results and Discussion

The derived BLSO thin films on LAO (001) substrates are relatively high quality and the resistivity, electronic mobility and optical transmittance at 300 K are $\sim 3 \text{ m}\Omega \text{ cm}$, $\sim 10 \text{ cm}^2\text{V}^{-1}\text{s}^{-1}$ and $> 75\%$ at 800 nm wavelength respectively, which are similar to our previous report.²³ Then, the BLSO thin films are prepared onto the transparent conducting BLSO/LAO substrates. The θ - 2θ XRD result of the all solution derived BFTO/BLSO/LAO (001) is shown in Fig. 1(a). It is seen that the diffraction peak from BLSO (002) can be clearly observed and no other diffraction peaks related with Sn element is observed, indicating the robustness of the derived BLSO thin film. Moreover, it is seen that the derived BFTO thin film is polycrystalline without preferred orientation and no undesirable phase is observed, suggesting the phase-pure characteristic of the derived BFTO thin film. As compared with the relatively strong diffraction peak intensity of BLSO thin film, the weak diffraction peak intensity of BFTO thin film can be attributed to the complex crystal structure of the BFTO. Figure 1(b) shows the glancing XRD result of the derived thin film with the standard XRD pattern, which further confirms the polycrystalline characteristic. The diffraction peaks can be well indexed to an orthorhombic lattice with the space group of $B2cb$, which is same as previous reports.^{10,15} The lattice constant is calculated by Bragg formula and the obtained lattice constant is of $a \sim 5.5 \text{ \AA}$, $b \sim 5.5 \text{ \AA}$ and $c \sim 49.6 \text{ \AA}$, which is similar to the previous reports indicating the stoichiometry of the derived BFTO thin film.^{12,15}

Figures 2(a) and 2(b) show the surface and cross-sectional FE-SEM results for the derived BFTO thin film, respectively. It is seen that the film is relatively dense with few pores and the grain size is about 100 nm and the root-mean roughness is about 50 nm as estimated from atomic force microscopy. As shown in Fig. 2(b), it is seen that the thickness of derived BFTO thin film is about 400 nm. Moreover, the interface between the BFTO and BLSO can be clearly seen, indicating the robustness of the BLSO bottom electrodes as previously report.¹⁷

Figure 3(a) shows the room-temperature leakage current density (J) in a semi-log scale on the electric field (E) for derived BFTO thin film. The asymmetric J - E can be attributed to the asymmetric electrodes. Moreover, the J is $1.1 \times 10^{-3} \text{ A/cm}^2$ at the positive 200 kV/cm electric field, which is smaller than the J of BFTO thin films on platinized silicon wafers,^{8,9,11,15} suggesting the advantages of BLSO bottom electrode. To investigate the leakage mechanisms, the J - E result is fitted and the results are shown in the inset of Fig. 3(a). It is seen that the double log J - E curve can be fitted by two linear segments with slope (s) values of ~ 1 and ~ 2 in low and high electric field region, respectively. The formation of the s value of 1 indicates an Ohmic conduction mechanism, in which the flow of electric current is mainly due to the thermally stimulated electrons.²⁵ The change in the s values from $s \sim 1$ to $s \sim 2$

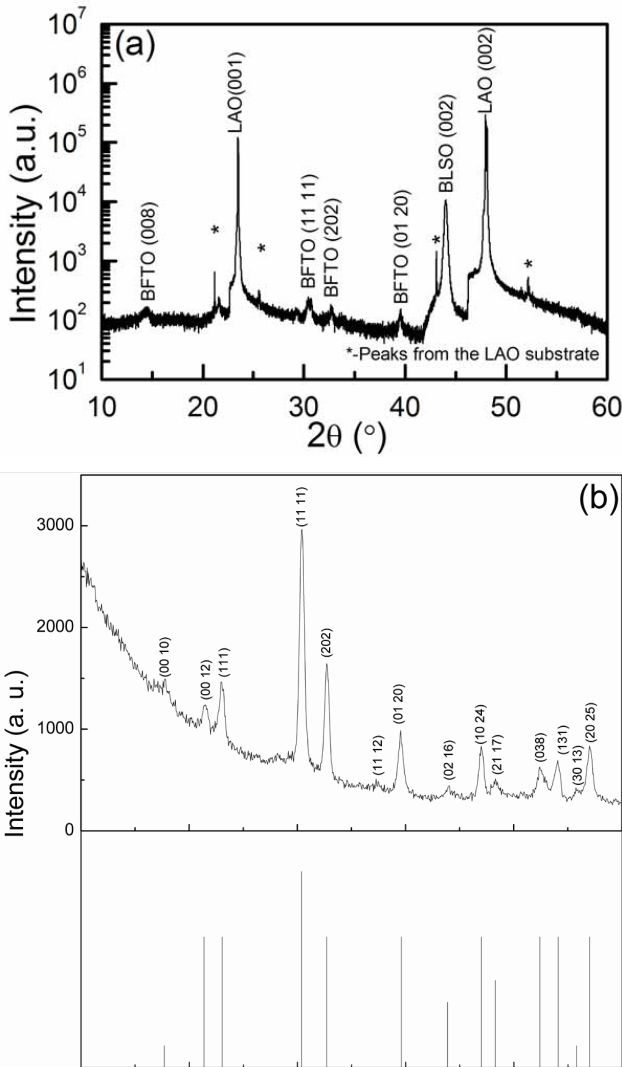


Fig. 1. (a) and (b) is XRD $\theta-2\theta$ and glancing XRD results, respectively.

indicates the existence of a space charge limited conduction (SCLC) mechanism, in which the concentration of free electrons due to carrier injection becomes greater than the concentration of thermally stimulated electrons.²⁶

Figure 3(b) shows the room-temperature electric field dependent ferroelectric polarization $P-E$ result at the measurement frequency of 2 kHz. It is seen that a well-defined $P-E$ hysteresis loop can be obtained and the remnant polarization $2P_r$ is of $\sim 16.8 \mu\text{C}/\text{cm}^2$ in the 500 kV/cm electric field and the coercive field $2E_c$ is 410 kV/cm. The obtained $2P_r$ is comparable to the reported values of BFTO

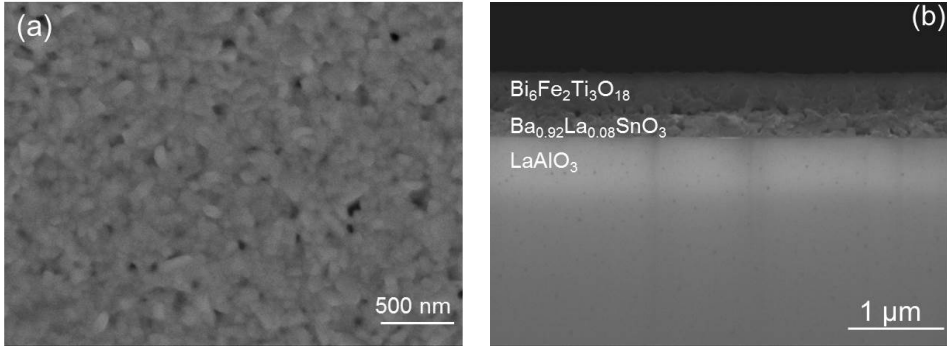


Fig. 2. (a) is the surface FE-SEM result and (b) is the cross-section FE-SEM result.

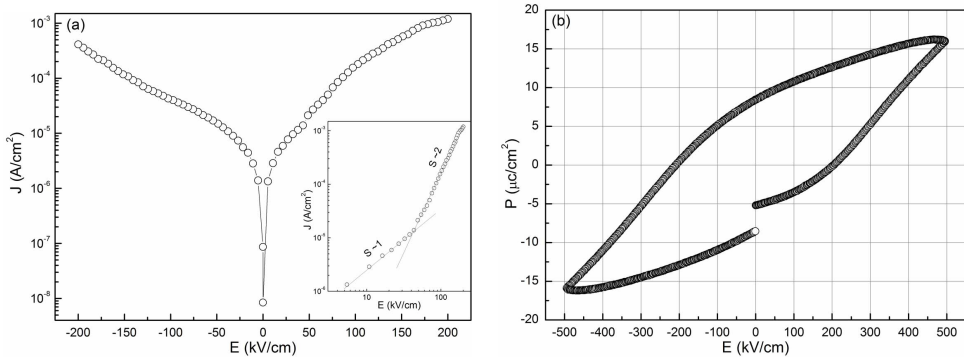


Fig. 3. (a) is the room-temperature $J-E$ in a semi-log scale and the inset shows the fitting results of the leakage and (b) shows the room-temperature $P-E$ hysteresis loop.

thin films by CSD processing on platinized silicon wafers,^{6,27,28} suggesting that BLSO thin films can be used as transparent conducting electrodes for BFTO thin films.

4. Conclusion

In summary, BFTO thin films on transparent conducting BLSO thin films as bottom electrodes were realized by all solution processing. The derived BFTO thin film is polycrystalline with dense microstructures. The remnant polarization $2P_r$ can reach $\sim 16.8 \mu\text{C}/\text{cm}^2$ in the 500 kV/cm electric field and the coercive field $2E_c$ is 410 kV/cm. The result will provide a feasible route to prepare BFTO thin films on transparent conducting bottom electrodes to realize multifunctionality.

Acknowledgment

This work was supported by the National Nature Science Foundation of China under contract Nos. 11104001 and 21271007.

References

1. H. N. Lee, D. Hesse, N. Zakarov and U. Gosele, *Science* **296** (2002) 2006.
2. A. Srinivas, S. V. Suryanarayana, G. S. Kumar and M. M. Kumar, *J. Phys.: Condens. Matter* **11** (1999) 3335.
3. W. Bai, G. Chen, J. Y. Zhu, J. Yang, T. Lin, X. J. Meng, X. D. Tang, C. G. Duan and J. H. Chu, *Appl. Phys. Lett.* **100** (2012) 082902.
4. E. Jartych, T. Pikula, M. Mazurek, A. Lisinska-Czekaj, D. Czekaj, K. Gaska, J. Przewoznik, C. Kapusta and Z. Surowiec, *J. Magn. Magn. Mater.* **342** (2013) 27.
5. A. Srinivas, D. W. Kim, K. S. Hong and S. V. Suryanarayana, *Mater. Res. Bull.* **39** (2004) 55.
6. J. W. Kim, C. M. Raghavan, J. Y. Choi, W. J. Kim, S. S. Kim and T. K. Song, *J. Korean Phys. Soc.* **66** (2015) 1344.
7. L. Zhang, G. Liu, Z. Tang, Y. Deng, J. Yu, X. Tang and X. Zhu, *J. Alloys Compd.* **650** (2015) 149.
8. C. M. Raghavan, J. W. Kim, J. W. Kim and S. S. Kim, *Ceram. Inter.* **40** (2014) 10649.
9. C. M. Raghavan, J. W. Kim, J. Y. Choi, S. S. Kim and J. W. Kim, *J. Sol-Gel Sci. Technol.* **73** (2015) 83.
10. H. Sun, B. W. Zou, X. R. Ni, X. Y. Mao, X. B. Chen and J. S. Zhu, *J. Mater. Sci.* **50** (2015) 5475.
11. C. M. Raghavan, J. W. Kim, J. Y. Choi, J. W. Kim and S. S. Kim, *Ceram. Inter.* **41** (2015) 3277.
12. W. Bai, W. F. Xu, J. Wu, J. Y. Zhu, G. Chen, J. Yang, T. Lin, X. J. Meng, X. D. Tang and J. H. Chu, *Thin Solid Films* **525** (2012) 195.
13. L. Keeney, T. Maity, M. Schmidt, A. Amann, N. Deepak, N. Petkov, S. Roy, M. E. Pemble and R. W. Whatmore, *J. Am. Ceram. Soc.* **96** (2013) 2339.
14. Z. Liu, J. Yang, X. W. Tang, L. H. Yin, X. B. Zhu, J. M. Dai and Y. P. Sun, *Appl. Phys. Lett.* **101** (2012) 122402.
15. D. P. Song, X. W. Tang, B. Yuan, X. Z. Zuo, J. Yang, L. Chen, W. H. Song, X. B. Zhu and Y. P. Sun, *J. Am. Ceram. Soc.* **97** (2014) 3587.
16. S. Kooriyattil, R. K. Katiyar, S. P. Pavunny, G. Morell and R. S. Katiyar, *Appl. Phys. Lett.* **015** (2014) 072908.
17. X. Luo, Y. S. Oh, A. Sirenko, P. Gao, T. A. Tyson, K. Char and S. W. Cheong, *Appl. Phys. Lett.* **100** (2012) 172112.
18. H. J. Kim, U. Kim, T. H. Kim, J. Kim, H. M. Kim, G. B. Jeon, W. J. Lee, H. S. Mun, K. T. Hong, J. Yu, K. Char and K. H. Kim, *Phys. Rev. B* **86** (2012) 165205.
19. J. H. Kim, U. Kim, H. M. Kim, T. H. Kim, H. S. Mun, B. G. Jeon, K. T. Hong, W. J. Lee, C. Ju and K. H. Kim, *Appl. Phys. Express* **5** (2012) 061102.
20. H. F. Wang, Q. Z. Liu, F. Chen, G. Y. Gao, W. Wu and X. H. Chen, *J. Appl. Phys.* **101** (2007) 106105.
21. P. V. Wadekar, J. Alaria, M. O'Sullivan, N. O. L. Flack, T. D. Manning, L. J. Phillips, K. Durose, O. Lozano, S. Lucas, J. B. Claridge and M. J. Rosseinsky, *Appl. Phys. Lett.* **105** (2014) 052104.
22. K. K. James, P. S. Krishnaprasad, K. Hasna and M. K. Jayaraj, *J. Phys. Chem. Solid* **76** (2015) 64.
23. R. H. Wei, X. W. Tang, Z. Z. Hui, X. Luo, J. M. Dai, J. Yang, W. H. Song, L. Chen, X. G. Zhu, X. B. Zhu and Y. P. Sun, *Appl. Phys. Lett.* **106** (2015) 101906.
24. C. Shan, T. Huang, J. Zhang, M. Han, Y. Li, Z. Hu and J. H. Chu, *J. Phys. Chem. C* **118** (2014) 6994.

25. C. Wang, M. Takahashi, H. Fujino, X. Zhao, E. Kume, T. Horiuchi and S. Sakai, *J. Appl. Phys.* **99** (2006) 054104.
26. A. Rose, *Phys. Rev.* **97** (1955) 1538.
27. A. Faraz, N. Deepak, M. Schmidt, M. E. Pemble and L. Keeney, *AIP Adv.* **5** (2015) 087123.
28. H. J. Kim, J. W. Kim, E. J. Kim, J. Y. Choi, C. M. Raghavan, W. J. Kim, M. H. Kim, T. K. Song, J. W. Kim and S. S. Kim, *Ferroelectrics* **465** (2014) 68.